Effects of a pupil filter on Stimulated Emission Depletion Microscopy

Hongki Yoo*[a], Incheon Song [a], Taehoon Kim [a], Daegab Gweon [a]

[a] Laboratory of Nano Opto-Mechatornics, Department of Mechanical Engineering,
Korea Advanced Institute of Science and Technology, Daejeon, Korea

ABSTRACT

Recently, stimulated emission depletion microscopy has achieved high resolution in fluorescent imaging. In this paper, we present effects of a pupil filter on the performances of stimulated emission depletion microscopy. In stimulated emission depletion microscopy, a saturated zero-centered spot is usually used to achieve a high lateral resolution. Using a half-coated phase plate, a zero-centered spot was made with a narrow and steep gap at the center. Numerical and experimental results show that by simply inserting a central obstacle as a pupil filter, it is possible to reduce the central gap of the zero-centered spot. However in order to compensate inevitable loss of light, which is blocked by the obstacle, increased laser power is required.

Keywords : STED microscopy, confocal microscopy, high resolution, pupil filter, phase plate, annular aperture.

1. INTRODUCTION

Far-field fluorescence confocal microscopy is a versatile tool for investigating biological specimens [1]. It is well known, however, that the resolution of light microscopy is limited by the wavelength and by the numerical aperture due to diffraction [2]. Recently, the lateral resolution and the axial resolution of fluorescence microscopy have been improved over the diffraction limits in stimulated emission depletion (STED) microscopy [3, 4]. STED microscopy uses synchronized excitation and STED pulses, whereby the wavelength of the latter is red-shifted from the emission peak of the fluorophore. The STED pulses suppress the spontaneous emission. Because the STED pulse forms a zero-centered spot, obtained by a half-coated phase plate [4, 5], the excited fluorophores are depleted, and little fluorescent light is emitted at the periphery of the diffraction-limited spot of the fluorescence confocal scanning microscopy. Thus, we can obtain fluorescent light only from the central region of the excited spot, which is much smaller than the diffraction limit.

An annular pupil filter is used to reduce the spot size and to suppress the sidelobes for achieving super-resolution in light microscopy [6-9]. A similar approach can be applied to STED microscopy. By simply inserting the central obstacle as a pupil filter in the STED beam path, it is possible to modify the pupil function, thus we can reduce the central gap of the zero-centered spot. This leads to a possible improvement of the spatial resolution of STED microscopy since the effective focal spot decreases as the central gap gets narrower. In this paper the effects of a pupil filter in STED microscopy is studied. We will present how the width of the obstacle affects both the central gap of the zero-centered spot and the light efficiency. They will be presented with the numerical and experimental results.

2. METHOD

In order to investigate how the pupil filter affects the performances of a stimulated emission depletion microscopy, numerical simulations and experiments are performed. Modifying the pupil function we can observe the changing shapes of the focal spots, thus the performance of a stimulated emission depletion microscopy can be analyzed and predicted.

* turtle99@kaist.ac.kr, phone 82-42-869-3265, fax 82-42-869-5225, http://nom.kaist.ac.kr/

Three-Dimensional and Multidimensional Microscopy: Image Acquisition and Processing XIII, edited by Jose-Angel Conchello, Carol J. Cogswell, Tony Wilson, Proc. of SPIE Vol. 6090, 60900X, (2006)
1605-7422/06/$15 · doi: 10.1117/12.647395

It is assumed that the light is unpolarized; thus, the scalar theory for the numerical simulations is applied. When the beam is focused by the lens, the light field at the image plane is expressed as [10]

$$U_2(x_2, y_2) = \frac{i}{\lambda} \iint_{-\infty}^{\infty} U_1(x_1, y_1) \exp[\frac{ik(x^2 + y^2)}{2f}] \frac{\exp(-ikr)}{r} \cos(\tilde{n}, \tilde{r}) \, dx_1 dy_1 , \qquad (1)$$

where $U_1(x_1, y_1)$ is the light field of the incidence light at the pupil plane, $U_2(x_2, y_2)$ is the light field at the image plane, λ is the wavelength of the light, f is the focal length of the lens, k is the wave number, r is the distance between (x_1, y_1) and (x_2, y_2), and $\cos(\tilde{n}, \tilde{r})$ is the angle between the wave vector and the observation direction. To calculate the transverse intensity point spread function (IPSF) of the STED spot, we start by considering the wavefront, half of which is delayed by $\pi/2$. Following this, inserting the central obstacle the light field at the pupil plane is expressed as

$$U_1(x_1, y_1) = \frac{1}{2}(1 + sign\,[\left|\frac{2x_1}{D_1}\right| - \varepsilon\,]) \times sign[x_1], \quad (x_1^2 + y_1^2)^{1/2} < \frac{D_1}{2}, \qquad (2)$$
$$= 0 \qquad , \quad otherwise,$$

where ε is the ratio of the aperture width (w) to the beam diameter (D_1), as shown in Fig. 1. The IPSF at the image plane is the modulus square of $U_2(x_2, y_2)$. Using Eqs. (1) and (2), the IPSFs are numerically calculated for different ε values. For this numerical simulation, MATLAB was used.

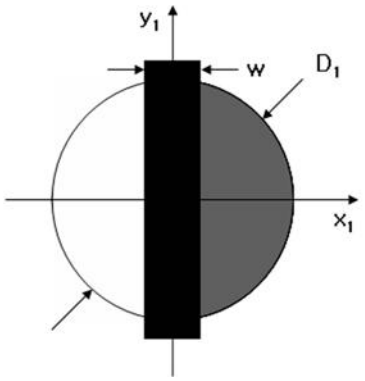

Fig. 1. The light field at the pupil plane with the phase plate and the central obstacle. U = -1 (white regions), 0 (black region), and 1 (gray region). D1 is the beam diameter and w is the width of the central obstacle

In order to demonstrate the effect of the central obstacle, we constructed the system shown in Fig. 2. For the light source, an unpolarized He-Ne laser at a wavelength of 543.5 nm was used. The light was delivered by an optical fiber and expanded by a collimator. The beam diameter was adjusted to 8 mm by a variable aperture iris, and the laser power was attenuated by an adjustable ND filter. We made a phase plate coated with MgF2 on half of one side in order to make a zero-centered spot. The other side of the phase plate was coated for an anti-reflection property. We also blocked the center of the phase plate with narrow white cards, which covered the edge of the coating, as the edge is not steep due to manufacturing-related reasons. Varying the width of the white cards, ε in Eq. 2 was adjusted. A doublet lens focused the light to make a spot at the focal plane. To obtain a magnified image of the focal spot, an objective lens of 40x and a CCD was used. We averaged 30 images to enhance the signal-to-noise ratio; additionally, the shutter speed was adjusted to use the full dynamic range of the CCD for the varying intensities. Modifying the pupil filter we can observe the varied spot shapes at the focal plane, thus we can analyze the effects of the pupil filter on the shape of the central gap and the peak intensity of the spot. Thus we can predict the performance of stimulated emission depletion microscopy with the pupil filter.

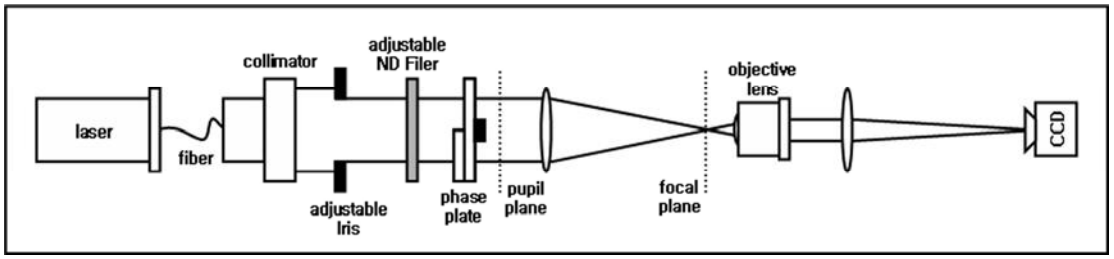

Fig. 2. Schematic diagram for the experiment.

3. RESULTS

Figure 3 shows the (a-d) numerically calculated and (e-h) experimentally measured STED IPSF with ε = 0.1 (a, e), 0.3(b, f), 0.5(c, g), and 0.7(d, h). The coordinates were normalized by an transverse optical coordinate [10] expressed as $v = 2\pi / \lambda \times D_1 / 2f \times r_1$, where $r_1 = (x_1^2 + y_1^2)^{1/2}$. The peak intensity was also normalized to the unity for the peak intensity value without pupil filter, i.e. when ε=0. As shown in the Fig. 3, STED IPSF has zero intensity at the center. Inner gap of IPSF gets narrower as the aperture ratio increases. Significant sidelobes were observed in the IPSF with larger aperture ratios. This will be further discussed later.

In Fig. 4, x-directional cross sections of the (a) theoretical and (b) experimental STED IPSFs are shown. The solid line, dashed line, dotted line, and dash-dot line shows the results with ε = 0.1, 0.3, 0.5, 0.7, respectively. In all cases, two main peaks and one central zero were clearly observed. The narrower gap is advantageous, as it reduces the effective IPSF of the STED microscopy. Table 1 shows the full width at half maximum (FWHM), which is determined by the width of the internal gap at half maximum intensity, and the light efficiency, η, which is determined by the ratio of the maximum intensity of the STED IPSF with a central obstacle to one without a central obstacle, according to various aperture ratios.

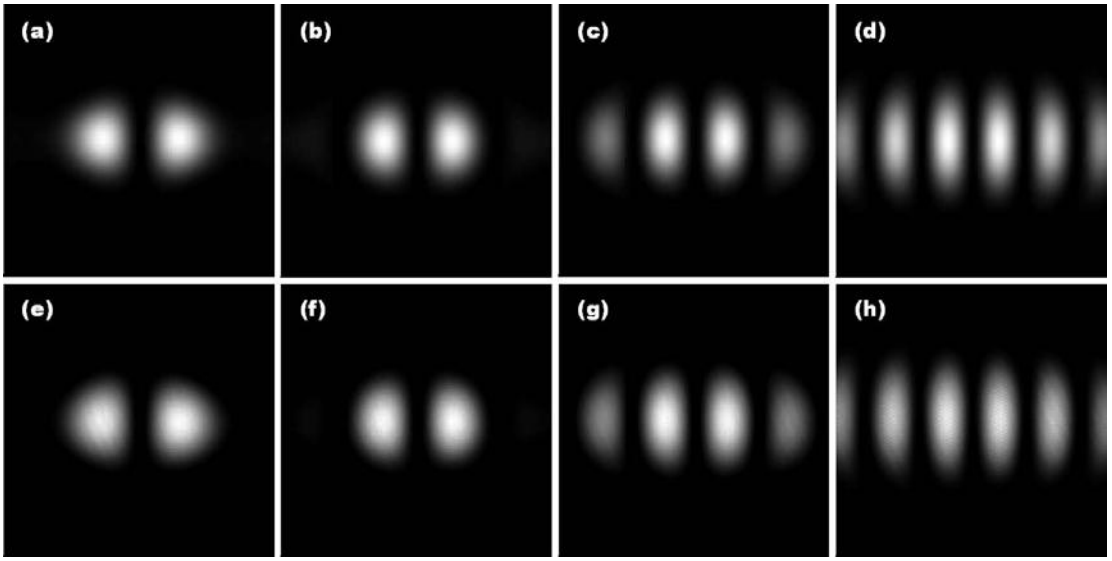

Fig. 3. (a-d) Numerically calculated and (e-h) experimentally measured STED IPSFs, with ε = 0.1 (a, e), 0.3(b, f), 0.5(c, g), and 0.7(d, h). Length of x and y is 20 optical units for all figures.

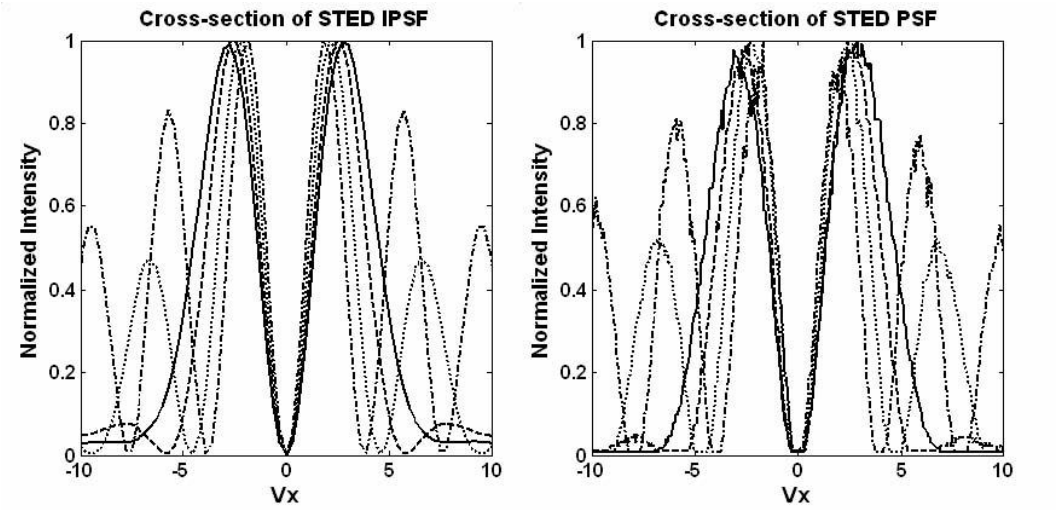

Fig. 4. x-directional cross sections of the (a) theoretical and (b) experimental STED IPSFs. The solid line, dashed line, dotted line, and dash-dot line shows the result with ε = 0.1, 0.3, 0.5, 0.7, respectively.

Aperture Ratio, ε	FWHM of Gap		Light Efficiency, η	
	Simulation	Experiment	Simulation	Experiment
0.1	2.74	2.70	0.94	0.94
0.3	2.47	2.58	0.56	0.58
0.5	2.16	2.18	0.21	0.22
0.7	1.88	1.92	0.04	0.05

Table. 1. FWHM of gap and light efficiency according to various aperture ratios.

When ε = 0.1, the FWHM of the gap was 2.74 for the numerical simulation and 2.70 for the experimental result. The FWHM of the gap was 2.16 and 2.18 in the numerical and experimental results, respectively, when ε = 0.5. It was about 20 percent smaller than the results when ε = 0.1. This means that it is possible to improve the lateral resolution of STED microscopy by 20 percent using the central obstacle with a width of half the beam diameter. However it is necessary to increase the laser power, since some of the STED beam is blocked by the central obstacle. This makes the intensity of the spot weaker. When ε = 0.5, the measured light efficiency was only 0.22. Thus, we should increase the laser power by a factor of 4.5 to maintain the maximum intensity of the focal spot, because intensity is an important factor for resolution in STED microscopy [11]. Although the laser power is strong, it does not induce the radiation problem, since the highest intensity that is radiated to the specimen is same.

Besides the gap narrowing or the light loss, we also observed the increasing sidelobes. In a typical case of a microscope with an annular aperture or a pupil filter, the additional sidelobes reduce any improvement of the resolution of the imaging system by adding unwanted artifacts to the images. As a result, a compromise is required between the enhancement of the resolution and the suppression of the sidelobes [8]. However, in the STED IPSF, the sidelobe is rarely a problem because the reduction of the effective IPSF depends on the narrow and steep gap between the two peaks. Accordingly the effects induced by the sidelobes can be ignored in any further analysis.

To investigate how the central obstacle affects the width of the two peaks at the STED IPSF, we obtained the relation between ε and the FWHM of the gap. In Fig. 5, the solid line shows the numerically calculated result, and the dotted line with crosses shows the experimentally measured result. Both results indicate that the central obstacle with the high aperture ratio produces the narrow gap of the two peaks. Unsurprisingly, the light efficiency decreases as the aperture ratio increases, as is shown in Fig. 6. For this reason, it is necessary to increase the laser power to compensate for the energy loss in order to fully achieve the advantage of the decreased gap of the two adjacent peaks of the STED IPSF. The compromise between the laser power and the FWHM of the gap depends on the available laser power and the required peak intensity of the STED spot for achieving the desired lateral resolution.

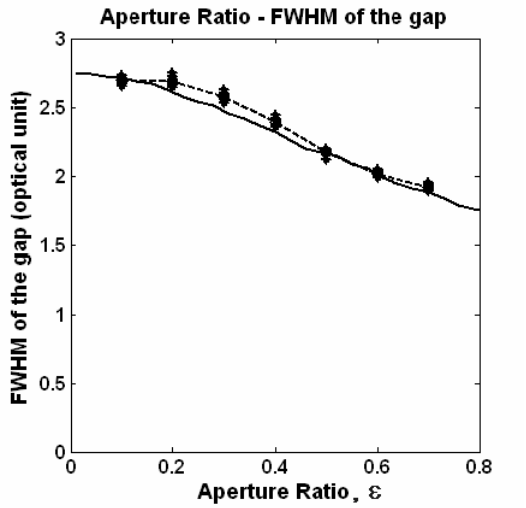

Fig. 5. The relation between the aperture ratio, ε and the internal FWHM of the gap of two peaks. The solid line shows the numerical simulation and the dotted line shows the experimental result.

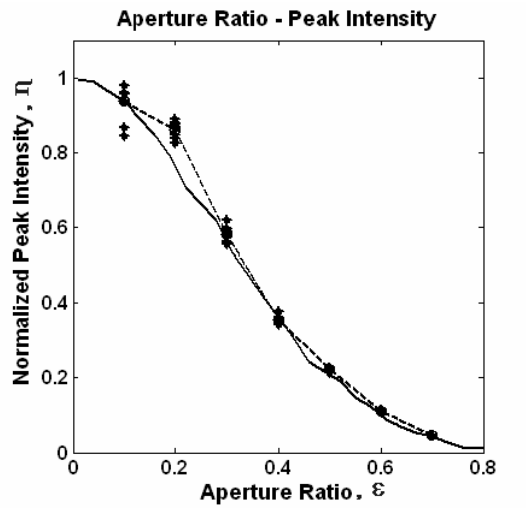

Fig. 6. The relation between the aperture ratio, ε and the light efficiency, η. The solid line shows the numerical simulation and the dotted line shows the experimental result.

4. DISCUSSION

In STED microscopy, zero-centered spot is essential for achieving high lateral resolution. Effects of a pupil filter, which blocks the central region of the STED beam, on the STED microscopy have been invested. The numerical calculations and the experimental results indicate that by inserting the central obstacle at the pupil plane, it is possible to reduce the internal gap of the two peaks at the STED IPSF, which is obtained by modifying the pupil function with the half-coated phase plate. In this case inevitable light loss occurs. Although the narrowing of the gap is achieved at the expense of being relatively light inefficient, it is possible to maintain the radiation energy by increasing the laser power without causing the radiation problem of the fluorescent specimen. This is easily achievable, because the typical laser power for the STED pulse is much lower than the power for the two-photon excitation, which is usually implemented with a femto-second laser. Overall, this means that we can improve the lateral resolution of STED microscopy. The

results show that the lateral resolution of STED microscopy can be improved by about 20% using the central obstacle with the reasonable drop of light efficiency.

5. ACKNOWLEDGEMENTS

This research was supported by the Korean Ministry of Commerce, Industry and Energy.

REFERENCES

1. J. B. Pawley, Handbook of Biological Confocal Microscopy (Plenum Press, New York, 1995).
2. M. Born and E. Wolf, Principles of Optics (Cambridge U. Press, Cambridge, UK, 1999).
3. S. W. Hell and J. Wichmann, "Breaking the Diffraction Resolution Limit by Stimulated Emission: Stimulated-Emission-Depletion Fluorescence Microscopy," Opt. Lett. 19, 780-782 (1994).
4. V. Westphal, L. Kastrup, and S. W. Hell, "Lateral Resolution of 28nm (Λ/25) in Far-Field Fluorescence Microscopy," App. Phys. B 77, 377-380 (2003).
5. H. Yoo, I. Song, and D. Gweon, "Measurement and Restoration of the Point Spread Function of Fluorescence Confocal Microscopy," J. Microsc. (To be published).
6. M. Gu, T. Tannous, and C. J. R. Sheppard, "Improved Axial Resolution in Confocal Fluorescence Microscopy Using Annular Pupils," Opt. Commun. 110, 533-539 (1994).
7. L. Liu, X. Deng, L. Yang, G. Wang, and Z. Xu, "Effect of an Annular Pupil Filter on Differential Confocal Microscopy," Opt. Lett. 25, 1711-1713 (2000).
8. M. A. A. Neil, R. Juŭkaitis, T. Wilson, Z. J. Laczik, and V. Sarafis, "Optimized pupil-plane filters for confocal microscope point-spread function engineering," Opt. Lett. 25, 245-247 (2000).
9. M. Martínez-Corral, A. Pons, and M. Caballero, "Axial Apodization in 4Pi-Confocal Microscopy by Annular Binary Filters," J. Opt. Soc. Am. A 19, 1532-1536 (2002).
10. M. Gu, Principles Of Three-Dimensional Imaging in Confocal Microscopes (World Scientific, Singapore, 1996).
11. T. A. Klar, E. Engel, and S. W. Hell, "Breaking Abbe's Diffraction Resolution Limit in Fluorescence Microscopy With Stimulated Emission Depletion Beams of Various Shapes," Phys. Rev. E 64, 066613 (2001).